

# Inhibition of the Insulin-Like Growth Factor I Receptor by Epigallocatechin Gallate Blocks Proliferation and Induces the Death of Ewing Tumor Cells

Hyung-Gyoo Kang<sup>1</sup>, Jasmine M. Jenabi<sup>1</sup>, Xian Fang Liu<sup>1</sup>, C. Patrick Reynolds<sup>2</sup>, Timothy J. Triche<sup>1</sup>, and Poul H.B. Sorensen<sup>1,3</sup>

## Abstract

The insulin-like growth factor I receptor (IGFIR) has emerged as a key therapeutic target in many human malignancies, including childhood cancers such as Ewing family tumors (EFT). In this study, we show that IGFIR is constitutively activated in EFTs and that the major catechin derivative found in green tea, (–)-epigallocatechin gallate (EGCG), can inhibit cell proliferation and survival of EFT cells through the inhibition of IGFIR activity. Treatment of EFT cell lines with EGCG blocked the autophosphorylation of IGFIR tyrosine residues and inhibited its downstream pathways including phosphoinositide 3-kinase-Akt, Ras-Erk, and Jak-Stat cascades. EGCG treatment was associated with dose- and time-dependent inhibition of cellular proliferation, viability, and anchorage-independent growth, as well as with the induction of cell cycle arrest and apoptosis. Apoptosis in EFT cells by EGCG correlated with altered expression of Bcl-2 family proteins, including increased expression of proapoptotic Bax and decreased expression of prosurvival Bcl2, Bcl-XL, and Mcl-1 proteins. Our results provide further evidence that IGFIR is an attractive therapeutic target in EFTs and that EGCG is an effective inhibitor of this receptor tyrosine kinase. EGCG may be a useful agent for targeting IGFIR, either alone or in combination, with other potentially more toxic IGFIR inhibitors for the management of EFTs. *Mol Cancer Ther*; 9(5); 1396–407. ©2010 AACR.

## Introduction

It is widely reported that catechin derivatives contained in green tea have antineoplastic activity (1). One of these compounds, (–)-epigallocatechin gallate (EGCG), is a major component of green tea and has long been known to inhibit carcinogenesis of diverse tumor types (2–5). Recent studies have shown potential chemotherapeutic efficacy of EGCG against cancers of the skin, lung, breast, colon, liver, stomach, and prostate (6–8). As with many other natural dietary substances that have been studied in recent years as potential anticancer agents, EGCG is attractive as a potential therapeutic due to its lack of significant toxicity in normal cells (9).

**Authors' Affiliations:** <sup>1</sup>Department of Pathology and Laboratory Medicine, Children's Hospital Los Angeles, Los Angeles, California; <sup>2</sup>Cancer Center, Texas Tech University Health Science Center School of Medicine, Lubbock, Texas; and <sup>3</sup>Department of Molecular Oncology, British Columbia Cancer Research Centre, Vancouver, British Columbia, Canada

**Note:** Supplementary materials for this article are available at Molecular Cancer Therapeutics Online (<http://mct.aacrjournals.org/>).

**Corresponding Author:** Poul H.B. Sorensen, Department of Molecular Oncology, British Columbia Cancer Research Centre, Room 4-112, Vancouver, British Columbia V5Z 1L4, Canada. Phone: 604-675-8202; Fax: 604-675-8218. E-mail: psor@interchange.ubc.ca

doi: 10.1158/1535-7163.MCT-09-0604

©2010 American Association for Cancer Research.

EGCG has been reported to inhibit a variety of cancer-related pathways including cell proliferation and tumor growth (2, 8), invasion and metastasis (3, 4), and angiogenesis and to induce apoptosis and cell cycle arrest of transformed cells (8, 10, 11). Although it remains unclear how EGCG mediates these biological responses, one proposed mechanism is through the inactivation of receptor tyrosine kinases (RTK). Recently, EGCG was shown to inhibit members of the epidermal growth factor receptor family including epidermal growth factor receptor and ErbB2 (12–14). EGCG has also been reported to inhibit the activation of vascular endothelial growth factor receptor (15), platelet-derived growth factor receptor (16), and insulin-like growth factor I receptor (IGFIR; ref. 17). Other potential targets for inhibition by EGCG include signaling by NF- $\kappa$ B in colon cancer cells (5), cyclooxygenase-2 expression and activity (18, 19), and matrix metalloproteinases such as matrix metalloproteinase-2 and matrix metalloproteinase-9 that are involved in tumor cell invasion and metastasis (20). This broad spectrum of mechanistic possibilities for the antineoplastic actions of EGCG supports the need for further studies to identify its relevant molecular targets. For example, this agent may have different targets depending on the cellular context and it will be essential to identify specific targets in a given tumor type to optimize potential clinical benefits of EGCG for that disease.

Ewing family tumors (EFT) are the second most frequent bone tumors in children and young adults, and can also occur in the soft tissues (21, 22). EFTs are characterized by specific gene fusions involving the *EWS* gene on chromosome 22 and erythroblastosis-26 (ETS)-related genes such as *FLI1* on chromosome 11 (23) or *ERG* on chromosome 21 (24). Many attempts have been made to elucidate the direct downstream targets that mediate transformation through EWS-FLI1 or EWS-ERG oncoprotein expression (25). Recently, new insights into the mechanism of EWS-ETS oncoproteins have been gleaned through more system-wide approaches (26). However, therapeutic targeting of EFT-associated chimeric transcription factors or their downstream pathways still remains extremely challenging.

In addition to EWS-ETS oncoproteins, EFTs are also reported to express several activated RTKs that likely contribute to the pathogenesis of EFT, including platelet-derived growth factor receptor, ERBB4, and IGFIR (27–29). Unlike chimeric transcription factors, RTKs are of interest therapeutically because of their potential druggability (30, 31). Recently, great interest has emerged in potentially targeting IGFIR in EFTs due to promise shown in early phase human clinical trials (29, 32, 33). Moreover, EWS-FLI1 requires the presence of IGFIR to transform mouse fibroblasts and IGFIR inhibition results in reduced tumorigenicity and metastasis of EFT cell lines (29). EWS-ETS fusion proteins induce IGFI promoter activity and an IGFI/IGFIR autocrine loop has been shown in EFTs (34, 35). EWS-FLI1 is also reported to repress *IGFBP3*, a negative regulator of IGFIR signaling (36). Finally, there is recent evidence that in childhood sarcomas, sensitivity to IGFIR blocking antibodies is linked to receptor levels (37). IGFIR is a transmembrane heterotrimer consisting of two  $\alpha$  and  $\beta$  subunits. The two major ligands for IGFIR are IGFs 1 and 2, and the biological activities of these ligands are themselves controlled by a family of IGF binding proteins (38). Ligand binding results in IGFIR autophosphorylation and the activation of several downstream signaling pathways including phosphoinositide 3-kinase (PI3K)-Akt, Ras-Erk, and Jak-Stat cascades. Here, we show that EGCG causes growth inhibition and the apoptosis of EFT cell lines and that this is associated with marked inhibition of IGFIR autophosphorylation and downstream signaling pathways.

## Materials and Methods

**Cell lines, tissue culture, and reagents.** Two EFT cell lines, TC32 and TC71, have previously been described (39, 40). Cells were grown in 5% CO<sub>2</sub> in RPMI supplemented with 10% fetal bovine serum, 2 mmol/L glutamine, 100 U/mL penicillin, and 100 mg/mL streptomycin (Life Technologies/Bethesda Research Laboratories). Human brain microvascular endothelial cells (HBMECs) were grown in the same condition. For anchorage-independent (spheroid) cultures, monolayer cells were trypsinized, resuspended as single cells, and

replated on tissue culture dishes coated with 1.5% agar as described (28, 41, 42). EGCG was purchased from Sigma. The Annexin V-FITC apoptosis detection kit was purchased from Beckman Coulter. IGFI and cyclolignan picropodophyllin (PPP) were purchased from R&D Systems and Calbiochem, respectively.

**Protein lysates, Western blotting, and immunoprecipitation.** Harvested cells were rinsed thrice in PBS containing 100  $\mu$ mol/L Na<sub>3</sub>VO<sub>4</sub> and then lysed in NP40 Lysis buffer (50 mmol/L HEPES, 100 mmol/L NaF, 10 mmol/L Na<sub>4</sub>P<sub>2</sub>O<sub>7</sub>, 2 mmol/L Na<sub>3</sub>VO<sub>4</sub>, 2 mmol/L EDTA, 2 mmol/L Na-MoO<sub>4</sub>, and 0.5% NP40) containing a commercial protease inhibitor cocktail (Roche) for 30 minutes at 4°C with shaking. Following solubilization, protein concentrations were quantitated using the DC Bio-Rad Protein assay kit (Bio-Rad Laboratories). Following electrophoretic transfer to Immobilon-P membranes (Millipore), Western blot analysis was done using the indicated antibodies, including rabbit anti-poly (ADP-ribose) polymerase (PARP) antibody, anti-phospho-AKT Ser-473, anti-total AKT, anti-phospho-mitogen-activated protein/extracellular signal-regulated kinase kinase 1/2 Ser-217/221, anti-Jak2, anti-Bcl2, anti-Bax and anti-phospho-IGFIR (Tyr-1132) antibodies (Cell Signaling), anti- $\beta$ -actin rabbit polyclonal antibody, anti-IGFIR rabbit polyclonal antibodies, (Santa Cruz), and 4G10 anti-phosphotyrosine mouse monoclonal antibodies (Upstate). Secondary anti-mouse and anti-rabbit horseradish peroxidase (HRP)-conjugated antibodies were from BD Transduction Laboratories. For immunoprecipitation, whole-cell lysates were prepared as above and 500  $\mu$ g cell lysates were precleared with Protein G agarose (Pierce) at 4°C for 1 hour. Precleared lysates were then incubated with appropriate antibodies overnight at 4°C. Protein G agarose was added to the mixture and incubated at 4°C for 1 hour. Beads were collected by centrifugation and washed thrice with the above lysis buffer. Proteins were eluted by boiling in SDS sample buffer and subjected to immunoblotting using appropriate antibodies.

**Cell cytotoxicity assays.** All cytotoxicity assays were done in 96-well tissue culture plates using a semiautomated digital image microscopy scanning system (DIMSCAN), which has a dynamic range of four logs of cell kill as described (28, 43). Briefly, TC32, TC71 cells, and HBMEC were plated at 5,000 cells with 100  $\mu$ L of complete medium per well. Cells were cultured for 1 day before the addition of concentration ranges of EGCG (0–100  $\mu$ mol/L; Sigma-Aldrich) in complete medium in replicates of 12 wells per condition. Plates were assayed 2 and 3 days after the initiation of EGCG treatment. To measure cytotoxicity, fluorescein diacetate was added to the plates to 10  $\mu$ g/mL and incubated for 20 minutes. Then, 30  $\mu$ L of eosin-Y (0.5% in normal saline) were added to quench background fluorescence (28, 43). Total fluorescence per well was then measured using a proprietary DIMSCAN system and results were expressed as the fractional survival of treated cells versus control cells. For apoptosis studies, spheroid and monolayer cells were

treated with different concentrations of EGCG (0–100  $\mu\text{mol/L}$ ). Following treatment of EGCG, harvested cells were lysed with the NP40 lysis buffer and caspase-3 activity assay or Western blotting were done using appropriate antibodies.

**Cell proliferation assays.** To investigate the effect of EGCG on cell proliferation, we used a bromodeoxyuridine (BrdUrd) cell staining kit (Calbiochem) according to the manufacturer's protocol. Briefly 5,000 cells were inoculated into 96-well plates and grew for 24 hours. Then, the cells were incubated with BrdUrd for 5 hours and fixed with fixative/denaturing solution. BrdUrd-incorporated cells were incubated with anti-BrdUrd antibody and detected with HRP-conjugated anti-mouse secondary antibody using tetra-methylbenzidine solution. Measurement of absorbance in each well was done using the GENiosPro instrument (Tecan) at 450 nm.

**Soft agar colony assays.** Soft agar assays were performed by seeding cells in triplicate at a concentration of 2,000 cells per well of six-well plates as previously described (28, 44). Plates were incubated for 14 days before being photographed and counted. Results shown are representative of three independent assays.

**Caspase-3 assays.** Caspase-3 activity was assayed by Z-DEVD-AFC cleavage according to the manufacturer's protocols (Calbiochem). Briefly, cells grown under the indicated conditions were lysed at 4°C and lysates were incubated with reaction buffer containing 50  $\mu\text{mol/L}$  Z-DEVD-AFC. After incubation at 37°C, fluorescence was measured with a GENiosPro instrument (Tecan). Caspase-3 activity was adjusted for protein concentration and relative activity was expressed as the fluorescence ratio between the normalized caspase-3 activity of non-treated cells (relative unit of 1.0) versus treated cells.

**Flow cytometry.** For the analysis of cell cycle, cells treated with or without EGCG were harvested, fixed with 70% ethanol, washed twice with PBS, and treated with RNase A. The fixed cells were stained with propidium iodide (PI). The fractions of different cell cycle cells were analyzed using BD LSR II flow cytometer (BD Biosciences) with the DiVA (version 4.1.2) software. To analyze apoptosis, cells were washed with PBS and incubated with anti-Annexin V-FITC (BD Biosciences) for 1 hour at room temperature. After washing cells with PBS, PI was added and the cells were incubated for 30 minutes. Then, the labeled cells were analyzed by flow cytometry.

**Activated RTK arrays.** TC32 and TC71 cells were grown for 48 hours in 10% serum-containing medium, followed by further 24 hours with or without 50  $\mu\text{mol/L}$  EGCG. Cells were then washed thrice with PBS containing 100  $\mu\text{mol/L}$   $\text{Na}_3\text{VO}_4$  and lysed in lysis buffer as previously described (28). Following lysis, 300  $\mu\text{g}$  of total protein was incubated with Human Phospho-RTK Arrays (R&D Systems) according to the manufacturer's protocols. Briefly, arrays were incubated with whole-cell lysates overnight at 4°C with shaking and washed with supplied washing buffer. Arrays were then incubated with anti-phosphotyrosine-HRP antibodies conjugated with HRP

for 2 hours at room temperature on a rocking platform shaker, before incubation with a chemiluminescent reagent and film exposure.

## Results

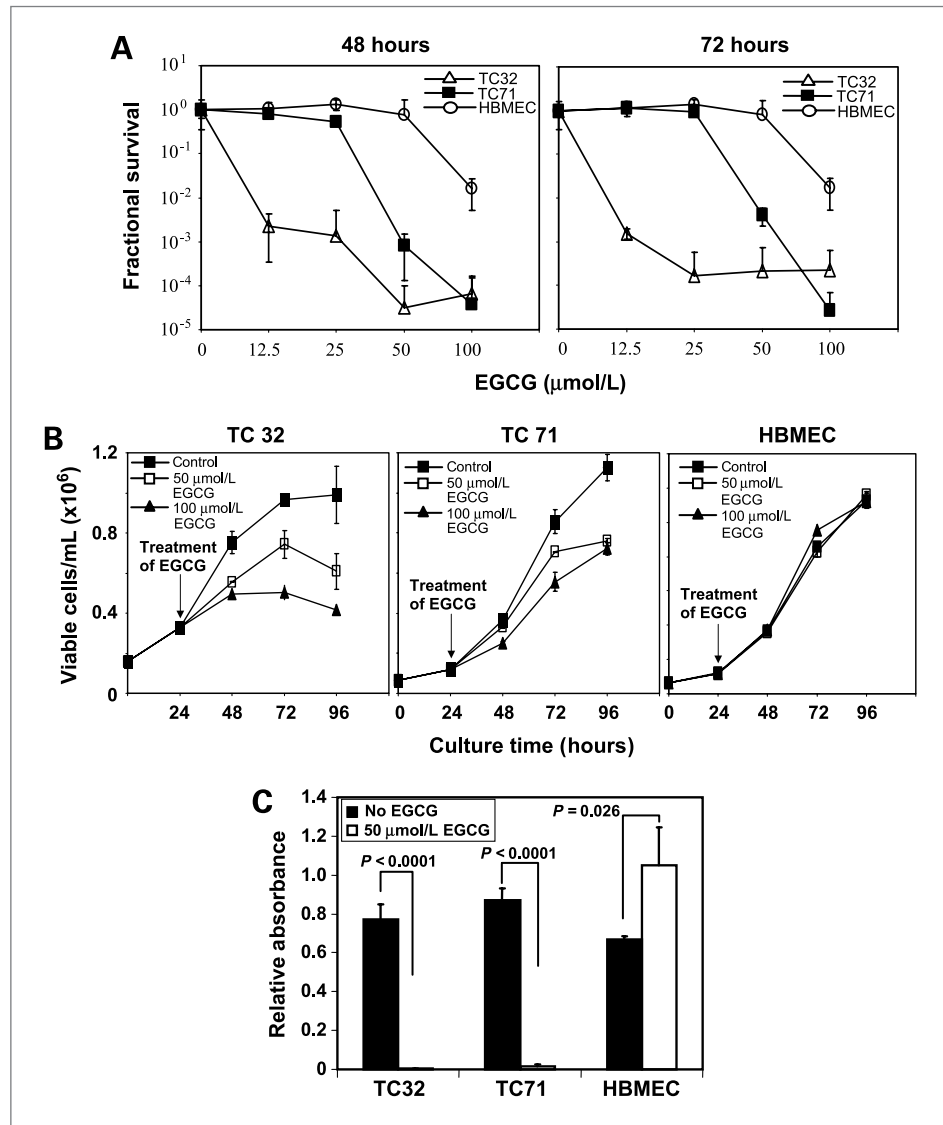
**EGCG induces cytotoxicity of EFT cells.** As a first step in evaluating the potential effects of EGCG on EFTs, we determined the cytotoxicity profiles of this agent against cultured TC32 and TC71 cells, two previously characterized EFT cell lines that both express the type I *EWS-FLI1* gene fusion (39, 40). Dose-dependent fractional survival of these and control normal HBMECs (45) in the presence and absence of EGCG was compared using the DIMSCAN drug sensitivity screening platform as previously described (28, 43). HBMECs were chosen as a controls as these are human and mesenchymal derived and have very low IGFIR levels (Supplementary Fig. S1A). EGCG treatment showed very weak cytotoxic effects on HBMEC cells and only at high (100  $\mu\text{mol/L}$ ) levels and this was evident even after 5 days. On the other hand, TC32 cells were sensitive at concentrations of 25  $\mu\text{mol/L}$  levels or less (Fig. 1A). TC71 cells were less sensitive than TC32 cells but still showed significant cytotoxicity at a 50  $\mu\text{mol/L}$  concentration. The reason for this discrepancy between TC32 and TC71 cells remains unknown. These results indicate that EFT cells are sensitive to EGCG treatment at concentrations that are ineffective at inducing cytotoxicity in normal HBMEC cells.

**EGCG inhibits growth of EFT cells.** We next wished to determine the effects of EGCG on EFT cell growth. TC32 and TC71 cells were treated with 0 to 100  $\mu\text{mol/L}$  EGCG over a time course of 0 to 96 hours and viable cell numbers were monitored. As shown in Fig. 1B, EGCG treatment produced moderate concentration-dependent inhibition of growth in both TC32 and TC71 cell lines but not in HBMECs. To further investigate effects on cell proliferation, all three cell lines were cultured in the presence of 50  $\mu\text{mol/L}$  EGCG for 24 hours and cell proliferation was determined by BrdUrd staining. As shown in Fig. 1C, EGCG dramatically inhibited BrdUrd uptake in EFT cell lines but not in HBMECs. These results indicate that EGCG has tumor-specific inhibitory effects on the proliferation of EFT cells.

**EGCG induces apoptosis of EFT cells.** We next determined whether the observed effects of EGCG on EFT cell growth are related to the induction of apoptosis. We first assessed morphologic changes of EFT cells treated with EGCG. As shown in Fig. 2A, EGCG treatment of TC32 and TC71 cells induced morphologic changes suggestive of apoptosis, including cell rounding and detachment from the plates. In contrast, these changes were not detected in EGCG-treated HBMECs. The proapoptotic effects of EGCG were further assessed by caspase-3 activation assays in cultures treated with varying concentrations of EGCG. As shown in Fig. 2B, caspase-3 activity showed a dose-dependent increase in TC32 and TC71 cells, which in contrast was not observed in HBMECs.

**Figure 1.** EGCG inhibits cell survival and growth of EFT cell lines but not of HBMECs. A, dose-responsive curves of fractional survival of EFT cells (TC32 and TC71) and HBMECs in the presence of EGCG. TC32, TC71, and HBMEC cells were grown in 96-well plates for 24 h and then treated with increasing concentrations of EGCG for 2 or 3 d as indicated. Fractional survival (cytotoxicity) profiles (with  $10^0$  designated as 100% survival) were determined by DIMSCAN analysis as described in Materials and Methods.

B, effects of EGCG on cell growth of TC32 and TC71 cell lines and HBMECs. Cells were grown in 96-well plates for 24 h and then treated with two concentrations of EGCG (50 and 100  $\mu\text{mol/L}$  as indicated) for different days. The proportion of viable cells was determined by exclusion of the Vi-Cell XR reagent (Beckman Coulter) as directed by the manufacturer. C, effects of EGCG on cell proliferation of TC32, TC71, and HBMEC lines. TC32, TC71, and HBMEC cells were grown in 96-well plates for 24 h and then treated with 50  $\mu\text{mol/L}$  EGCG for a further 12 h. Cells were then incubated with BrdUrd for 5 h and BrdUrd incorporation was determined by staining with anti-BrdUrd antibodies, followed by detection with anti-mouse antibodies conjugated to HRP as described in Materials and Methods.



Moreover, we observed marked cleavage of PARP, a well-known caspase-3 substrate, in EFT cells but not in HBMECs after 24 hours of EGCG treatment (Fig. 2C). Flow cytometry was then done to examine effects of EGCG on the cell cycle of EFT cells. As shown in Fig. 3A, EGCG treatment caused only minimal alterations in cell cycle profiles of TC32 or TC71 cells, with slight accumulation of treated cells in the  $G_0$ - $G_1$  phase. In contrast, when TC32 cells (and TC71 cells; data not shown) were analyzed by Annexin V and PI staining, there was a dramatic increase in apoptotic cells following EGCG treatment (Fig. 3B), which was not observed in HBMECs (Fig. 3C). The percentage of apoptotic TC32 cells increased in a dose-dependent fashion, with  $\sim 90\%$  apoptotic cells after treatment with 25  $\mu\text{mol/L}$  EGCG. These results indicate that the predominant effect of EGCG on EFT cells may be through the induction of apoptosis,

with a possible minor effect in inducing cell cycle arrest. Therefore, EGCG specifically induces EFT cell apoptosis.

**EGCG inhibits the anchorage-independent growth of EFT cells.** We next examined the effects of EGCG on the anchorage-independent growth of EFT cells using soft agar colony assays. As shown in Fig. 4A and B, TC32 and TC71 cells treated with two different concentrations of EGCG (50 and 100  $\mu\text{mol/L}$ ) showed a dose-dependent reduction in the size and number of colonies in soft agar. Similar to the cytotoxicity results of Fig. 1, TC32 were more sensitive than TC71 cells to EGCG treatment in these assays. We also analyzed EGCG effects on anchorage-independent growth by culturing cells on agar-coated plates as described to induce multicellular spheroid formation (28). As shown in Supplementary Fig. S1B, spheroid formation was dramatically reduced in the presence of 50  $\mu\text{mol/L}$  EGCG. This correlated with

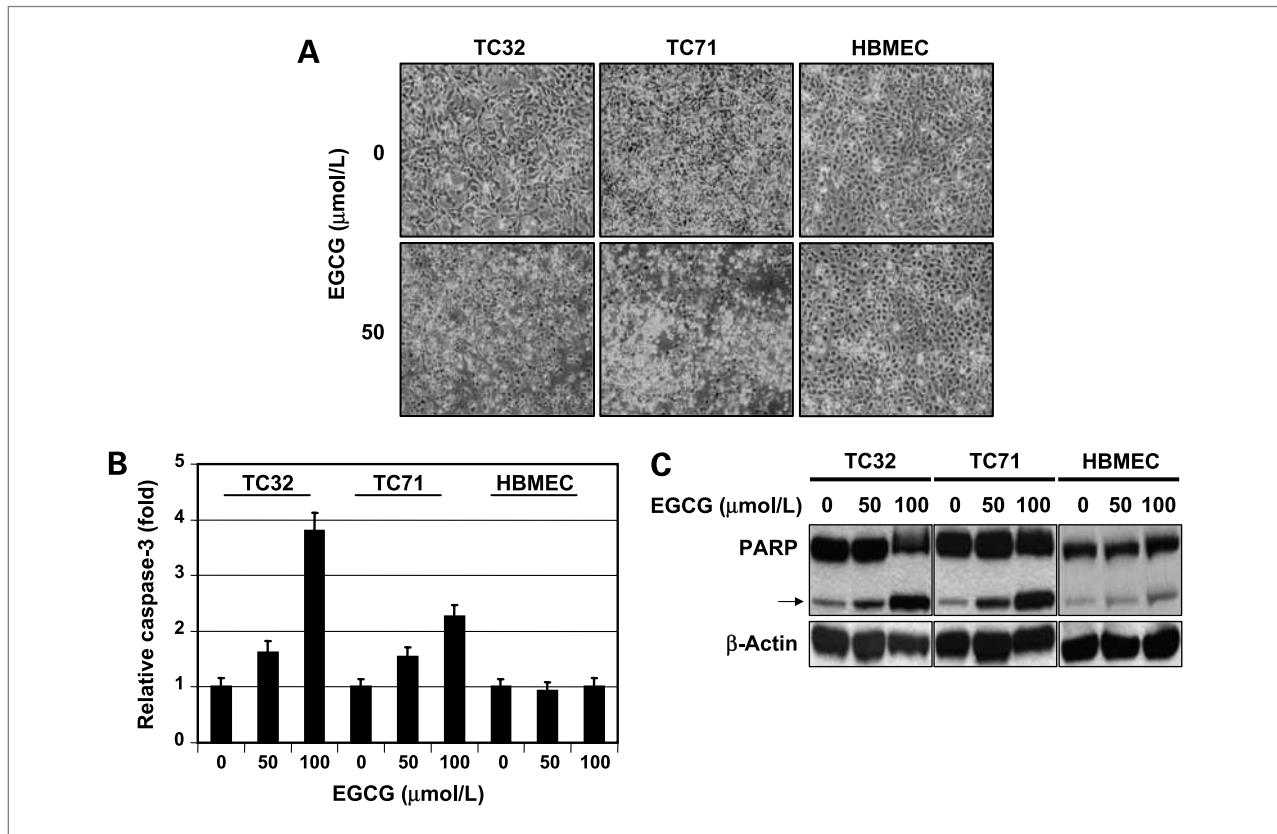


**Figure 2.** EGCG induces apoptosis of TC32 and TC71 cells but not HBMECs. TC32, TC71, and HBMEC were grown for 24 h and then treated with different concentrations of EGCG for 12 h. **A**, effects of EGCG on morphology of TC32, TC71, and HBMEC cells. Cells were photographed using a phase-contrast microscope (magnification,  $\times 100$ ). **B**, caspase-3 activity was measured in cell lysates by fluorometry using caspase-3 cleavage kits as described in Materials and Methods, adjusting for protein concentration and normalized to a value of 1.0 arbitrary unit for nontreated cells. **C**, lysates from cells treated with EGCG (0, 50, and 100  $\mu\text{mol/L}$ ) were assayed for PARP cleavage by Western blotting using antibodies to PARP. Arrowhead, cleaved PARP.  $\beta$ -Actin was used as a loading control.

a marked increase in caspase-3 activity in EGCG-treated cells (Supplementary Fig. S1C). Taken together, these results indicate that the target of EGCG in EFT cells might not only be involved in cell survival of EFT monolayer cells but also in anchorage-independent cell growth and survival.

**EGCG inhibits PI3K-Akt and Ras-Erk signaling and alters the expression of Bcl-2 family proteins in EFT cells.** To test which signaling pathways might be targeted as part of the mechanism of action of EGCG, we first assessed the effects of EGCG on the PI3K-Akt and Ras-Erk pathways, two cascades that are well known to mediate tumor cell growth and survival. To do this, we monitored the activation states of molecules involved in these pathways by Western blot analysis using phospho-specific antibodies. As shown in Fig. 4C, treatment of TC32 and TC71 cells with EGCG resulted in a dose-dependent reduction of phospho-Akt (Ser-473) and, to a lesser extent, phospho-Erk1/2, as read-outs of PI3K-Akt and Ras-Erk signaling, respectively. In contrast, Akt and Erk1/2 phosphorylation was unaffected by treatment of HBMECs with EGCG, indicating that EGCG selectively inhibits PI3K-Akt

and Ras-Erk signaling in EFT cells. Because EGCG treatment of TC32 and TC71 cells predominantly induces apoptosis (see above), we next compared potential downstream effector molecules of PI3K-Akt and/or Ras-Erk pathways that regulate apoptosis. Bcl-2 family proteins consist of both proapoptotic and prosurvival molecules, and homodimerization and heterodimerization of these proteins play key roles in the transduction and integration of apoptosis (46). We therefore examined the expression of a panel of Bcl-2 family proteins known to be regulated through PI3K-Akt and/or Ras-Erk pathways. As shown in Fig. 4C, treatment of EFT cells with EGCG resulted in a dose-dependent reduction of prosurvival members such as Bcl-2, Bcl-XL, and Mcl-1, whereas expression of the proapoptotic Bax protein was induced by EGCG treatment. These results provide preliminary evidence that EGCG-mediated induction of apoptosis in EFT cells may involve alterations in Bcl-2 family proteins and that this may occur through inhibition of PI3K-Akt and/or Ras-Erk signaling.

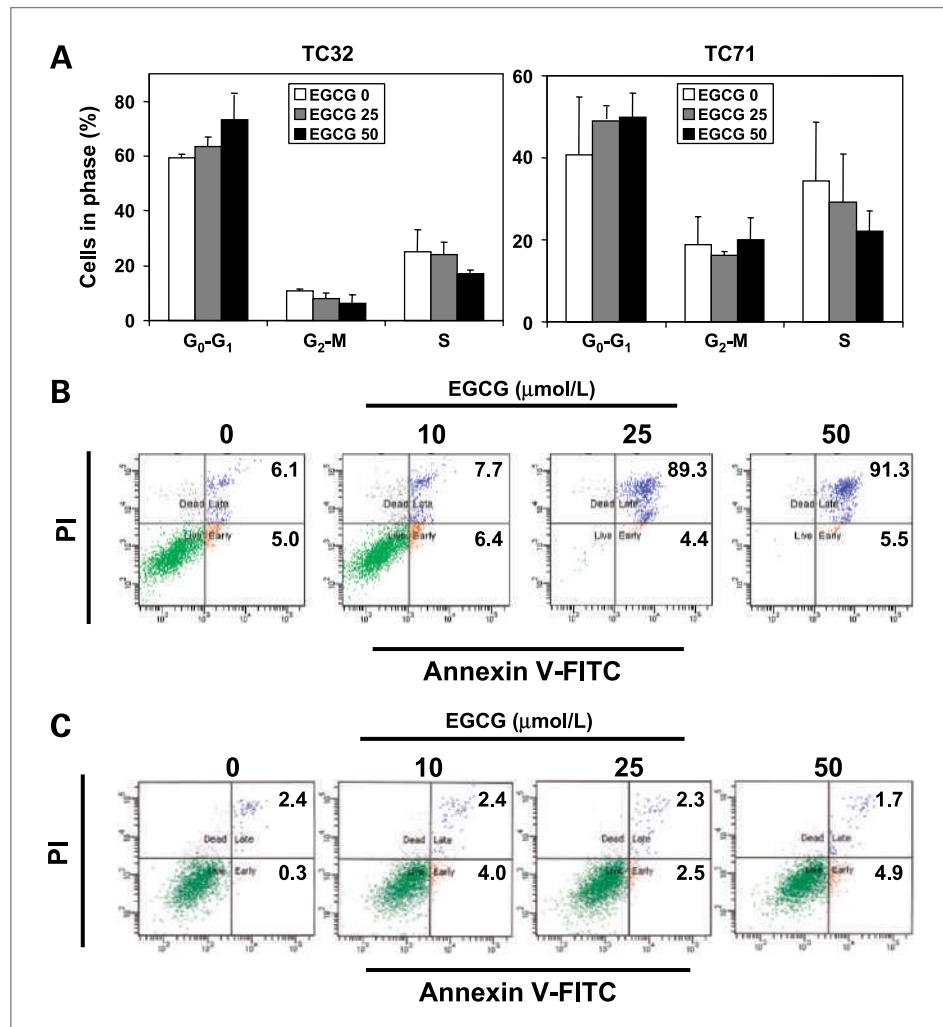
**EGCG inhibits IGF1R activation in EFT cells.** Because EGCG inhibits both PI3K-Akt and Ras-Erk signaling in

EFT cells, we wondered whether this agent might be targeting specific RTKs in EFT cells, particularly because this agent has been reported to block RTKs (1). To test this, we used the R&D Systems Human Phospho-RTK Antibody Proteome Profiler Array of 42 different tyrosine kinases (47), which we previously used to screen for RTK activation in EFT cell lines (28). Lysates from TC32 and TC71 cell lines grown in 10% serum-containing media with or without EGCG showed reduced activation of several RTKs in 50  $\mu\text{mol/L}$  EGCG-treated cells. Of these, the most prominent reduction in RTK tyrosine phosphorylation in both cell lines was observed for IGFIR (see Fig. 5A). To validate this, TC32 and TC71 lysates were subjected to IGFIR immunoprecipitation followed by immunoblotting with anti-phosphotyrosine antibodies. This showed dramatic decreases in IGFIR tyrosine phosphorylation in EGCG-treated compared with non-treated cells, whereas total IGFIR levels were unchanged (Fig. 5B). Identical results were obtained when cells were first serum starved overnight and then stimulated with 50 ng/mL IGF1 for 3 hours in the presence or absence of

EGCG. As shown in Fig. 5C, exogenous IGF1 stimulated IGFIR phosphorylation, but this was almost completely blocked by treatment with EGCG. As a positive control, we also treated cells with PPP, a known inhibitor of IGFIR in diverse tumor types (48). As shown in Supplementary Fig. S2A and B, treatment of TC32 and TC71 cells with increasing levels of PPP showed dose-dependent increases in caspase-3 activation and PARP cleavage as *in vitro* markers of apoptosis. Similar to EGCG, PPP treatment correlated with the loss of IGFIR tyrosine phosphorylation (Supplementary Fig. S2C). In contrast, PPP had no significant effects on cell growth or apoptosis of HBMECs (data not shown). Although our findings do not rule out the effects of EGCG and PPP on other pathways, they are consistent with these agents directly or indirectly targeting IGFIR.

To independently validate that effects of EGCG on transformed mesenchymal cells are indeed related to blocking the IGFIR pathway, we used a different model system to study this process. We previously identified the ETV6-NTRK3 (EN) chimeric tyrosine kinase as a

**Figure 3.** EGCG induces  $G_1$  cell cycle arrest and apoptosis in a dose-dependent fashion in TC32 and TC71 cells. **A**, effects of EGCG on cell cycle distribution in TC32 and TC71 cells. Cells were treated with EGCG (25 and 50  $\mu\text{mol/L}$ ) for 12 h, and cell cycle was analyzed with standard flow cytometry after PI staining as described in Materials and Methods. **B** and **C**, effects of EGCG on apoptosis in TC32 (**B**) and HBMEC cells (**C**). TC32 and HBMEC were treated with EGCG (0–50  $\mu\text{mol/L}$ ) for 12 h, and cells were stained with PI and anti-Annexin V antibodies. Cells were analyzed by flow cytometry. Numbers in each box, the percentage of cells in early apoptosis (low PI/high Annexin V cells; bottom right boxes) or in late apoptosis (hi PI/high Annexin V; top right boxes) as described in Materials and Methods.



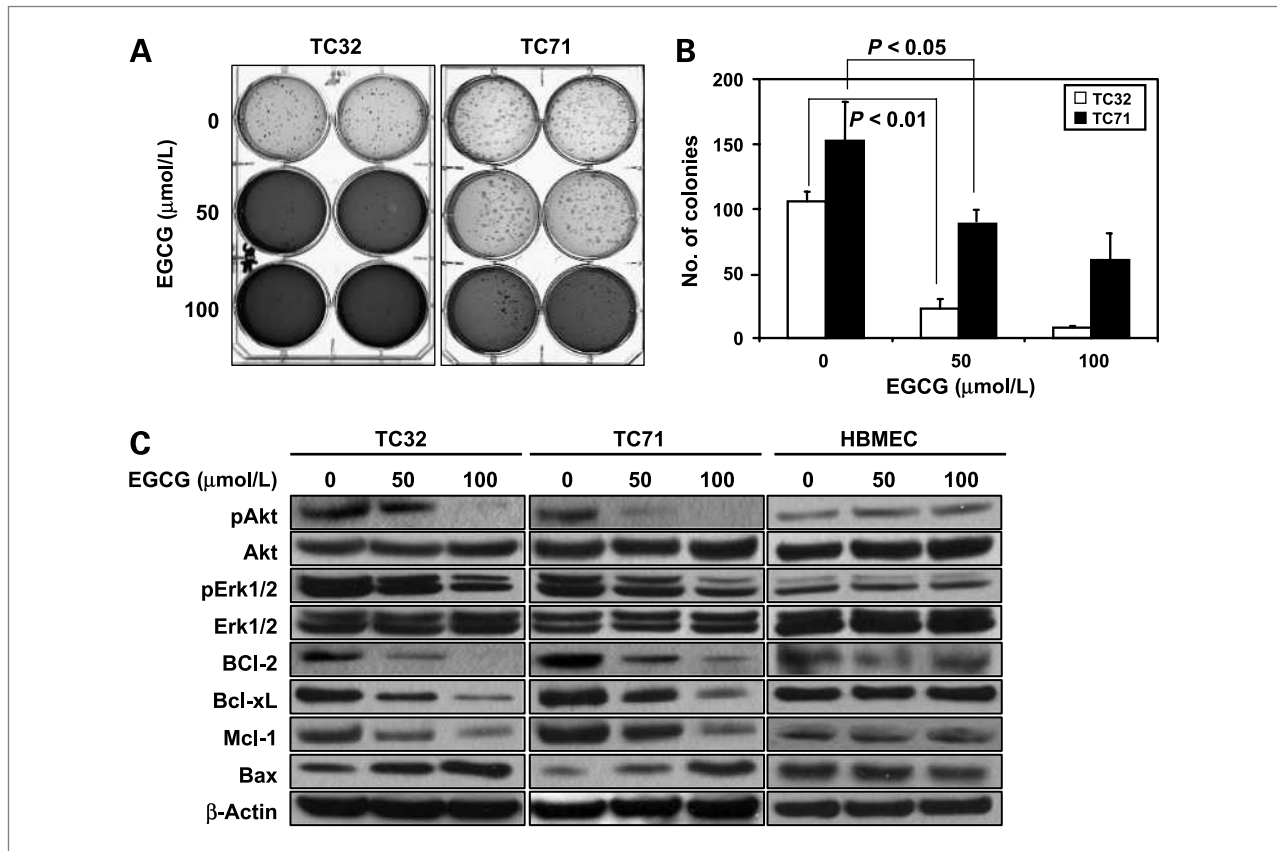


**Figure 4.** Effects of EGCG on the anchorage-independent growth of EFT cells. A and B, EGCG impairs colony formation of TC32 and TC71 cells in soft agar. Cells were grown in soft agar for 14 d as described in Materials and Methods. After 14 d, plates were photographed (A) and the colonies were counted (B). Columns, representative of three replicate wells for each condition. Statistical analysis was done by Student's *t* test. C, effects of EGCG on the activation and expression of apoptotic and cell cycle regulatory proteins in TC32 and TC71 cells and HBMECs. TC32, TC71, and HBMEC cells were grown for 24 h and then treated with EGCG (50 and 100 μmol/L) for 12 h. Cells were lysed and subjected to immunoblotting with antibodies to the indicated proapoptotic and antiapoptotic proteins. β-Actin was used as a loading control.

transforming oncoprotein in congenital fibrosarcoma (49) and secretory breast cancer (50). EN requires a functional IGFIR axis for transformation (42, 51) and is incapable of transforming mouse embryo fibroblasts lacking IGFIR (so-called R<sup>-</sup> cells). However, EN transformation is restored when R<sup>-</sup> cells are engineered to reexpress IGFIR (so-called R<sup>+</sup> cells; ref. 42). We previously showed that when EN is constitutively membrane targeted using a myristoylation tag (designated ENmyr), then cells no longer require IGFIR for transformation and the ENmyr mutant is capable of transforming R<sup>-</sup> cells (42). We therefore compared the EGCG sensitivity of R+EN cells (IGFIR+/EN+) versus R-ENmyr cells (IGFIR-/ENmyr+; Supplementary Fig. S3A), both of which are transformed (42). As shown in Supplementary Fig. S3B, EGCG induces caspase-3 activation only in R+EN (and R+ control cells) but not in IGFIR-deficient R-ENmyr cells. Moreover, EGCG only blocks the soft agar colony formation of R+EN cells and not R-ENmyr cells, which lack IGFIR (Supplementary Fig. S3C and D). Neither R+, as shown, nor R-EN cells (data not shown) formed colonies in soft

agar, as previously reported (42). Collectively, these data provide compelling evidence that the observed EGCG cytotoxic effect on transformed mesenchymal cells is related to IGFIR expression.

**EGCG blocks Jak2/Stat1/3/5 signaling in EFT cells.** As additional evidence that EGCG targets IGFIR signaling, we next examined whether, in addition to PI3K-Akt and Ras-Erk cascades (Fig. 4C), EGCG inhibits other known downstream effector pathways of IGFIR. Recent studies suggest cross-talk between IGFIR signaling and the Jak-Stat pathway and that IGFIR can activate the Jak2-Stat3 cascade (52–54). We therefore examined whether EGCG could modulate Jak-Stat signaling in EFT cells. As shown in Supplementary Fig. S2D, EGCG strongly inhibited tyrosine phosphorylation of Jak2, Stat1, Stat3, and Stat5, whereas Stat2 and Stat6 were unaffected. Jak2-Stat signaling was not activated in HBMEC lines (data not shown). Although this does not prove that IGFIR inhibition by EGCG directly blocks Jak2-Stat activation, our data provide preliminary evidence for an IGFIR-Jak2-Stat1/3/5 axis in EFT cells that is inhibited by EGCG.

**EGCG inhibits IGFIR in other childhood sarcomas.** We next wished to determine whether EGCG inhibits IGFIR signaling in childhood sarcomas other than EFTs. We therefore treated the rhabdomyosarcoma cell lines, HR and JR, and the osteosarcoma cell lines, OST and SaOS2, with 0 to 100  $\mu\text{mol/L}$  EGCG and assessed cellular responses as described above. EGCG inhibited cell proliferation (Fig. 6A) and induced apoptosis of each of these cell lines in a dose-dependent fashion (Fig. 6B and C), although there was variability in the responses among the cell lines. Next, we examined whether these effects of EGCG correlate with inhibition of IGFIR as observed for EFT cell lines. As shown in Fig. 6D, EGCG inhibited the activation of IGFIR, although again with some variability among cell lines. These results provide preliminary evidence that EGCG can inhibit IGFIR in a potentially broader spectrum of childhood sarcoma cells.

## Discussion

The polyphenol catechin EGCG is a major component of green tea that has been a worldwide dietary component for over 5,000 years (55). EGCG has variably been reported to possess antioxidant, antimutagenic, antidiabetic, anti-inflammatory, antibacterial, and anticancer properties. Epidemiologic research has shown that the frequency of green tea consumption correlates with reduced rates of cancer development or recurrence in

diverse tumor types, including breast cancer (56). Although the exact targets of EGCG remain unknown, it is currently thought to modify the activities of various RTKs and/or signal transduction pathways acting downstream of these proteins (1). Clearly, a better understanding of the fundamental mechanism of action of EGCG is needed to more effectively use this compound as a cancer therapeutic or preventive agent, particularly in combination with other therapeutics (9, 55). To our knowledge, EGCG has not yet been tested in childhood sarcomas such as EFTs. Here, we show that in the well-established EFT cell lines, TC32 and TC71, EGCG treatment led to marked growth inhibition, induction of apoptosis, and a block in activation of the IGFIR pathway at micromolar concentrations. EGCG treatment led to the inhibition of Ras-Erk, PI3K-Akt, and Jak2-Stat signaling in EFT cells; to the loss of expression of the prosurvival factors Bcl-2, Bcl-XL, and Mcl-1; and to the increased expression of the proapoptotic Bax protein.

In normal cells, expression and activation of RTKs and their ligands are precisely regulated, but in many cancers, these controls are lost or altered. Therefore, RTKs or other activated protein tyrosine kinases are considered as attractive therapeutic targets in tumor cells (31). However, many currently available RTK inhibitors, including small-molecule kinase inhibitors and blocking antibodies, have significant toxicities (57). Therefore, a low toxicity agent such as EGCG that augments RTK inhibition

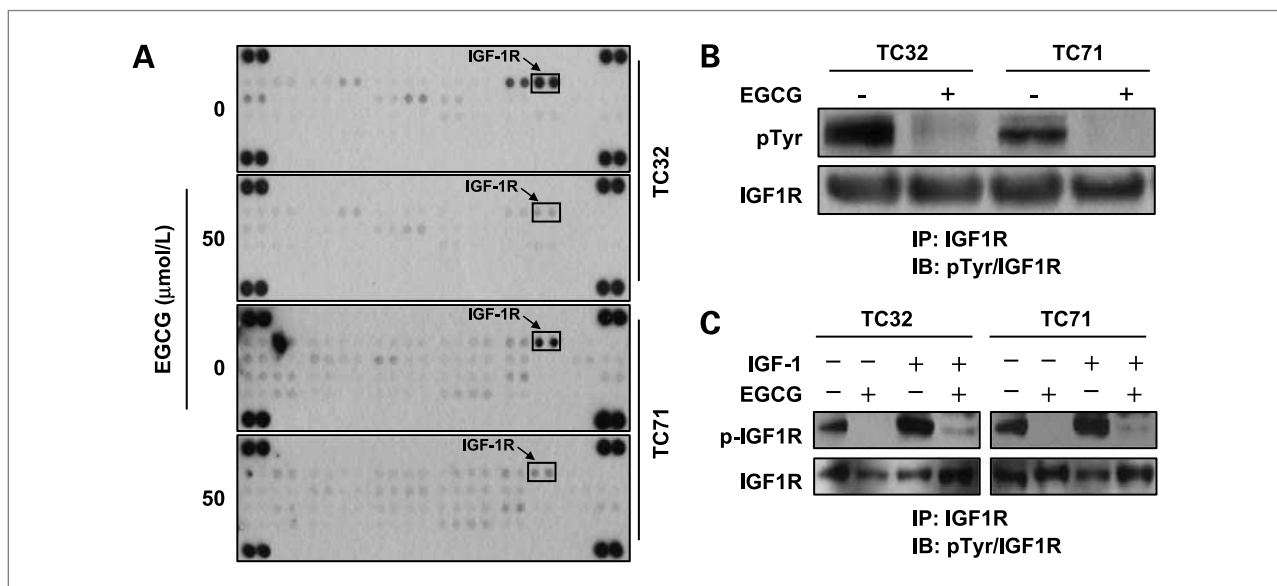


**Figure 5.** EGCG impairs IGFIR activation in EFT cells. **A**, the R&D Systems Human Phospho-RTK Antibody Proteome Profiler Array system was used to see the EGCG effect on activation of specific tyrosine kinases in TC32 and TC71 cells. Lysates from cells treated with (50  $\mu\text{mol/L}$ ) or without EGCG (0  $\mu\text{mol/L}$ ) were incubated with membranes arrayed with antibodies to 42 different tyrosine kinases as described by the manufacturer. Membranes were then washed and incubated with anti-phosphotyrosine antibodies, followed by enhanced chemiluminescence detection to identify activated tyrosine kinases. Boxes, the positions of anti-IGFIR antibodies. **B**, lysates from TC32 and TC71 cultures treated with or without EGCG (50  $\mu\text{mol/L}$ ) were subjected to immunoprecipitation using antibodies to IGFIR, followed by immunoblotting (IB) with 4G10 anti-phosphotyrosine (PTyr) antibodies or anti-IGFIR antibodies as indicated. **C**, TC32 and TC71 cells were first serum starved overnight in the presence or absence of EGCG (50  $\mu\text{mol/L}$ ) and then stimulated with 50 ng/mL of IGF-1 for 3 h. The cells were lysed and lysates were subjected to immunoprecipitation (IP) with anti-IGFIR antibodies and then immunoblotted with 4G10 anti-phosphotyrosine or anti-IGFIR antibodies as indicated.



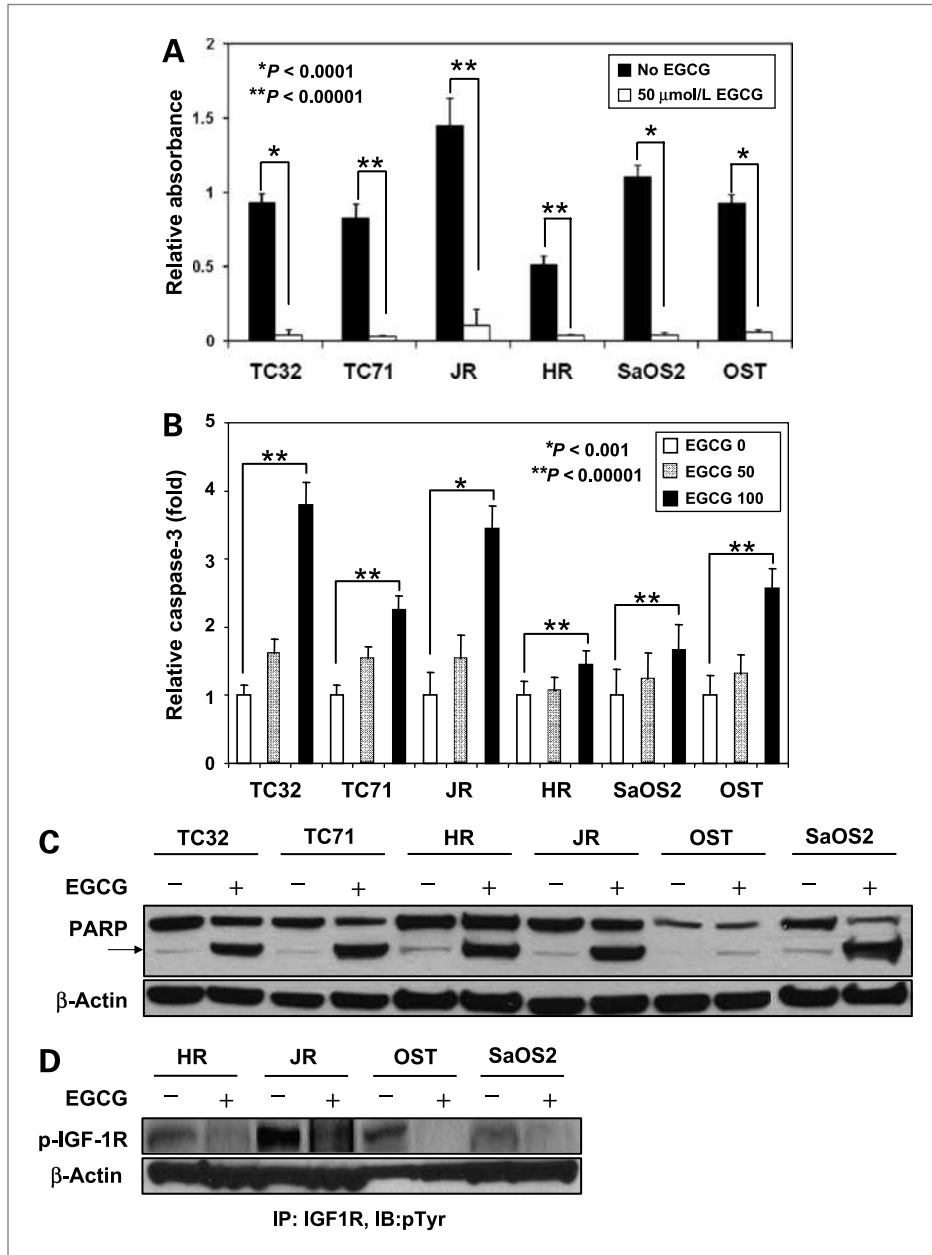


**Figure 6.** Effects of EGCG on cell proliferation and apoptosis of rhabdomyosarcoma cells (JR and HR) and osteosarcoma cells (SaOS2 and OST). **A**, cells were grown in 96-well plates for 24 h and then the cells were treated with 50 µmol/L EGCG for 12 h. Cells were then incubated with BrdUrd for 5 h and proliferation was measured by BrdUrd incorporation using anti-BrdUrd antibodies as described in Fig. 1C. **B**, cells were grown for 24 h and then treated with vehicle or two concentrations of EGCG (50 and 100 µmol/L) for 12 h. Cell lysates were then isolated and caspase-3 activity was measured by fluorometry as described in Fig. 2A, after adjusting for protein concentration. Values were normalized to a value of 1.0 arbitrary unit for nontreated cells. **C**, lysates from the same cells were assayed for PARP cleavage by standard Western blotting using anti-PARP antibodies. Arrowhead, cleaved PARP. β-Actin was used as a loading control. **D**, lysates from cells treated with or without 50 µmol/L EGCG for 24 h were subjected to immunoprecipitation (IP) using antibodies to IGF1R followed by immunoblotting (IB) with 4G10 anti-phosphotyrosine antibodies.

would be highly desirable. In a screen for tyrosine kinases that might be targeted by EGCG in EFTs, we found that IGF1R is highly activated in EFTs under 10% serum growth conditions and that EGCG dramatically blocks IGF1R tyrosine phosphorylation. Moreover, Ras-Erk, PI3K-Akt, and Jak-Stat1/3/5 pathways, which are known downstream cascades of IGF1R, were also blocked by EGCG. Similar results were observed with the PPP, a well-established IGF1R inhibitor. In contrast, effects were not observed in nontransformed HBMECs, whose IGF1R expression levels are much lower than in EFT cell lines (Supplementary Fig. S1A). These studies

support the notion that EGCG either directly or indirectly targets IGF1R in these cells.

IGF1R has previously been suggested as a potential target for EGCG. Recently, it was shown that the IGF1R binds EGCG in R- mouse embryo fibroblast cells, derived from mice with a targeted disruption of the *Igf1R* locus, once these cells were engineered to reexpress IGF1R (so-called R+ cells; ref. 58). EGCG had little or no effect on the growth of parental R- cells, but expression of IGF1R restored the sensitivity of the cells to EGCG-mediated apoptosis (58). In that study, it was also reported that EGCG could directly inhibit the kinase

activity of IGFIR through competitive binding to the ATP binding pocket of the IGFIR protein. We therefore performed cytotoxicity assays of EGCG using R- and R+ cells stably expressing the EN chimeric tyrosine kinase, generated by the t(12;15) translocation of congenital fibrosarcoma and secretory breast cancer, or an EN mutant, ENmyr, which is constitutively targeted to the plasma membrane (42). Although EN is incapable of transforming R- cells, similar to most known dominantly acting oncoproteins (59), membrane-targeted ENmyr no longer requires IGFIR for transformation and can transform both R- and R+ cells (42). EGCG only blocks the soft agar colony formation of R+EN cells whereas R-ENmyr cells were unaffected by EGCG treatment (as were R+ENmyr cells; data not shown). These studies provide strong evidence that EGCG cytotoxicity of EFT and potentially other sarcoma cells is functioning through the inhibition of IGFIR or a component of the IGFIR pathway. However, our data also do not address whether IGFIR is a direct *in vivo* target of EGCG in EFT cells or whether EGCG is targeting EFT cells because they are highly IGFIR dependent. Recent evidence suggests that IGFIR may be the major activator of the PI3K-Akt pathway in childhood sarcoma cells and therefore these tumors would be expected to be susceptible to an agent that blocks the IGFIR pathway. It is also conceivable that EGCG targets other RTKs, common downstream components of multiple RTKs, or activates a phosphatase negatively regulating IGFIR (and/or other RTKs). Indeed, we found that the Janus kinase Jak2 as well as its downstream effectors Stat1, Stat3, and Stat5 (but not Stat2 or Stat6) are activated in EFTs and that this process is blocked by EGCG. Jak-Stat signaling is involved in diverse cellular processes including proliferation, survival, and differentiation (60). Tyrosine phosphorylation of Stat3 has been described in EFTs (61), but to our knowledge Jak-Stat signaling has not been otherwise evaluated in these tumors. Although EGCG may target Jak2 directly, several studies suggest that tyrosine phosphorylation of Jak2 and Stat3 is induced by IGFI-mediated activation of IGFIR (52–54). Therefore, the effects of EGCG on Jak2-Stat signaling may then, through its ability to block IGFIR, inhibit the down-

stream Jak2-Stat3 cascade. Further studies are required to elucidate whether the inhibition of Jak-Stat signaling by EGCG is dependent on IGFIR inhibition.

We also tested the effects of EGCG on other childhood sarcoma cell lines, including rhabdomyosarcoma (JR and HR) and osteosarcoma (OST and SaOS2) cell lines. Similar to EFT cells, EGCG treatment resulted in a block in proliferation, increased apoptosis, and loss of IGFIR tyrosine phosphorylation in these cell types. Although preliminary, our data suggest that EGCG should be evaluated as a potential therapeutic in a broader spectrum of childhood sarcomas. In the present study, we observed *in vitro* efficacy at concentrations of 25 to 100  $\mu\text{mol/L}$ . Although this range is several orders of magnitude higher than is desirable for most molecular therapeutics, the low toxicity profile of EGCG may allow for clinical use. In particular, EGCG may be of benefit in combination with other RTK small-molecule inhibitors or blocking antibodies such as those targeting IGFIR. Inclusion of EGCG in the treatment of EFT with other IGFIR inhibitors might then allow for decreased dosing of the latter in therapeutic regimens, leading to lower overall toxicity profiles.

#### Disclosure of Potential Conflicts of Interest

No potential conflicts of interest were disclosed.

#### Acknowledgments

We thank Dr. Stuart Siegel for support and helpful discussions.

#### Grant Support

Ronald A. and Victoria Mann Simms Foundation, the Fannie Ripple Foundation, the David Paul Kane Foundation, and the Melanie Silverman Bone and Soft Tissue Fund (P.H.B. Sorensen), and U.S. Department of Defense grant W81XWH-07-1-0580 (P.H.B. Sorensen, C.P. Reynolds, and T.J. Triche).

The costs of publication of this article were defrayed in part by the payment of page charges. This article must therefore be hereby marked *advertisement* in accordance with 18 U.S.C. Section 1734 solely to indicate this fact.

Received 07/01/2009; revised 03/09/2010; accepted 03/09/2010; published OnlineFirst 04/27/2010.

#### References

- Khan N, Afaq F, Saleem M, Ahmad N, Mukhtar H. Targeting multiple signaling pathways by green tea polyphenol (–)-epigallocatechin-3-gallate. *Cancer Res* 2006;66:2500–5.
- Adhami VM, Malik A, Zaman N, et al. Combined inhibitory effects of green tea polyphenols and selective cyclooxygenase-2 inhibitors on the growth of human prostate cancer cells both *in vitro* and *in vivo*. *Clin Cancer Res* 2007;13:1611–9.
- Lim YC, Park HY, Hwang HS, et al. (–)-Epigallocatechin-3-gallate (EGCG) inhibits HGF-induced invasion and metastasis in hypopharyngeal carcinoma cells. *Cancer Lett* 2008;271:140–52.
- Shankar S, Ganapathy S, Hingorani SR, Srivastava RK. EGCG inhibits growth, invasion, angiogenesis and metastasis of pancreatic cancer. *Front Biosci* 2008;13:440–52.
- Shimizu M, Deguchi A, Hara Y, Moriwaki H, Weinstein IB. EGCG inhibits activation of the insulin-like growth factor-1 receptor in human colon cancer cells. *Biochem Biophys Res Commun* 2005;334:947–53.
- Lu YP, Lou YR, Xie JG, et al. Topical applications of caffeine or (–)-epigallocatechin gallate (EGCG) inhibit carcinogenesis and selectively increase apoptosis in UVB-induced skin tumors in mice. *Proc Natl Acad Sci U S A* 2002;99:12455–60.
- Witschi H, Espiritu I, Ly M, Uyeminami D, Morin D, Raabe OG. Chemoprevention of tobacco smoke-induced lung tumors by inhalation of an epigallocatechin gallate (EGCG) aerosol: a pilot study. *Inhal Toxicol* 2004;16:763–70.
- Siddiqui IA, Malik A, Adhami VM, et al. Green tea polyphenol EGCG sensitizes human prostate carcinoma LNCaP cells to TRAIL-mediated apoptosis and synergistically inhibits biomarkers

- associated with angiogenesis and metastasis. *Oncogene* 2008;27:2055–63.
9. Verschoyle RD, Steward WP, Gescher AJ. Putative cancer chemopreventive agents of dietary origin-how safe are they? *Nutr Cancer* 2007;59:152–62.
  10. Syed DN, Afaq F, Kweon MH, et al. Green tea polyphenol EGCG suppresses cigarette smoke condensate-induced NF- $\kappa$ B activation in normal human bronchial epithelial cells. *Oncogene* 2007;26:673–82.
  11. Amin AR, Thakur VS, Paul RK, et al. SHP-2 tyrosine phosphatase inhibits p73-dependent apoptosis and expression of a subset of p53 target genes induced by EGCG. *Proc Natl Acad Sci U S A* 2007;104:5419–24.
  12. Adachi S, Nagao T, To S, et al. (-)-Epigallocatechin gallate causes internalization of the epidermal growth factor receptor in human colon cancer cells. *Carcinogenesis* 2008;29:1986–93.
  13. Somers-Edgar TJ, Scandlyn MJ, Stuart EC, Le Nedelec MJ, Valentine SP, Rosengren RJ. The combination of epigallocatechin gallate and curcumin suppresses ER  $\alpha$ -breast cancer cell growth *in vitro* and *in vivo*. *Int J Cancer* 2008;122:1966–71.
  14. Sah JF, Balasubramanian S, Eckert RL, Rorke EA. Epigallocatechin-3-gallate inhibits epidermal growth factor receptor signaling pathway. Evidence for direct inhibition of ERK1/2 and AKT kinases. *J Biol Chem* 2004;279:12755–62.
  15. Rodriguez SK, Guo W, Liu L, Band MA, Paulson EK, Meydani M. Green tea catechin, epigallocatechin-3-gallate, inhibits vascular endothelial growth factor angiogenic signaling by disrupting the formation of a receptor complex. *Int J Cancer* 2006;118:1635–44.
  16. Park JS, Kim MH, Chang HJ, et al. Epigallocatechin-3-gallate inhibits the PDGF-induced VEGF expression in human vascular smooth muscle cells via blocking PDGF receptor and Erk-1/2. *Int J Oncol* 2006;29:1247–52.
  17. Shimizu M, Shirakami Y, Sakai H, et al. EGCG inhibits activation of the insulin-like growth factor (IGF)/IGF-1 receptor axis in human hepatocellular carcinoma cells. *Cancer Lett* 2008;262:10–18.
  18. Hussain T, Gupta S, Adhami VM, Mukhtar H. Green tea constituent epigallocatechin-3-gallate selectively inhibits COX-2 without affecting COX-1 expression in human prostate carcinoma cells. *Int J Cancer* 2005;113:660–9.
  19. Ahmed S, Rahman A, Hasnain A, Lalonde M, Goldberg VM, Haqqi TM. Green tea polyphenol epigallocatechin-3-gallate inhibits the IL-1  $\beta$ -induced activity and expression of cyclooxygenase-2 and nitric oxide synthase-2 in human chondrocytes. *Free Radic Biol Med* 2002;33:1097–105.
  20. Fassina G, Vene R, Morini M, et al. Mechanisms of inhibition of tumor angiogenesis and vascular tumor growth by epigallocatechin-3-gallate. *Clin Cancer Res* 2004;10:4865–73.
  21. Khoury JD. Ewing sarcoma family of tumors. *Adv Anat Pathol* 2005;12:212–20.
  22. Kovar H. Context matters: the hen or egg problem in Ewing's sarcoma. *Semin Cancer Biol* 2005;15:189–96.
  23. Delattre O, Zucman J, Plougastel B, et al. Gene fusion with an ETS DNA-binding domain caused by chromosome translocation in human tumours. *Nature* 1992;359:162–5.
  24. Sorensen PH, Lessnick SL, Lopez-Terrada D, Liu XF, Triche TJ, Denny CT. A second Ewing's sarcoma translocation, t(21;22), fuses the EWS gene to another ETS-family transcription factor, ERG. *Nat Genet* 1994;6:146–51.
  25. Riggi N, Stamenkovic I. The biology of Ewing sarcoma. *Cancer Lett* 2007;254:1–10.
  26. Kauer M, Ban J, Kofler R, et al. A molecular function map of Ewing's sarcoma. *PLoS ONE* 2009;4:e5415.
  27. Zwerner JP, May WA. Dominant negative PDGF-C inhibits growth of Ewing family tumor cell lines. *Oncogene* 2002;21:3847–54.
  28. Kang HG, Jenabi JM, Zhang J, et al. E-cadherin cell-cell adhesion in ewing tumor cells mediates suppression of anoikis through activation of the ErbB4 tyrosine kinase. *Cancer Res* 2007;67:3094–105.
  29. Martins AS, Ordonez JL, Garcia-Sanchez A, et al. A pivotal role for heat shock protein 90 in Ewing sarcoma resistance to anti-insulin-like growth factor 1 receptor treatment: *in vitro* and *in vivo* study. *Cancer Res* 2008;68:6260–70.
  30. Daub H, Specht K, Ullrich A. Strategies to overcome resistance to targeted protein kinase inhibitors. *Nat Rev Drug Discov* 2004;3:1001–10.
  31. Gschwind A, Fischer OM, Ullrich A. The discovery of receptor tyrosine kinases: targets for cancer therapy. *Nat Rev Cancer* 2004;4:361–70.
  32. Yeh J, Litz J, Hauck P, Ludwig DL, Krystal GW. Selective inhibition of SCLC growth by the A12 anti-IGF-1R monoclonal antibody correlates with inhibition of Akt. *Lung Cancer* 2008;60:166–74.
  33. Ludwig JA. Ewing sarcoma: historical perspectives, current state-of-the-art, and opportunities for targeted therapy in the future. *Curr Opin Oncol* 2008;20:412–8.
  34. Scotlandi K, Benini S, Sarti M, et al. Insulin-like growth factor I receptor-mediated circuit in Ewing's sarcoma/peripheral neuroectodermal tumor: a possible therapeutic target. *Cancer Res* 1996;56:4570–4.
  35. Cironi L, Riggi N, Provero P, et al. IGF1 is a common target gene of Ewing's sarcoma fusion proteins in mesenchymal progenitor cells. *PLoS ONE* 2008;3:e2634.
  36. Prieur A, Tirode F, Cohen P, Delattre O. EWS/FLI-1 silencing and gene profiling of Ewing cells reveal downstream oncogenic pathways and a crucial role for repression of insulin-like growth factor binding protein 3. *Mol Cell Biol* 2004;24:7275–83.
  37. Cao L, Yu Y, Darko I, et al. Addiction to elevated insulin-like growth factor I receptor and initial modulation of the AKT pathway define the responsiveness of rhabdomyosarcoma to the targeting antibody. *Cancer Res* 2008;68:8039–48.
  38. Martins AS, Mackintosh C, Martin DH, et al. Insulin-like growth factor I receptor pathway inhibition by ADW742, alone or in combination with imatinib, doxorubicin, or vincristine, is a novel therapeutic approach in Ewing tumor. *Clin Cancer Res* 2006;12:3532–40.
  39. Sorensen PHB, Liu XF, Thomas G, et al. Reverse transcriptase PCR amplification of EWS/FLI-1 fusion transcripts as a diagnostic test for peripheral primitive neuroectodermal tumors of childhood. *Diag Mol Pathol* 1993;2:147–57.
  40. Sorensen PH, Liu XF, Delattre O, et al. Reverse transcriptase PCR amplification of EWS/FLI-1 fusion transcripts as a diagnostic test for peripheral primitive neuroectodermal tumors of childhood. *Diagn Mol Pathol* 1993;2:147–57.
  41. Lawlor ER, Scheel C, Irving J, Sorensen PHB. Anchorage-independent multi-cellular spheroids as an *in vitro* model of growth signaling in Ewing tumors. *Oncogene* 2002;21:307–18.
  42. Martin MJ, Melnyk N, Pollard M, et al. The insulin-like growth factor I receptor is required for Akt activation and suppression of anoikis in cells transformed by the ETV6-NTRK3 chimeric tyrosine kinase. *Mol Cell Biol* 2006;26:1754–69.
  43. Keshelava N, Frgala T, Krejsa J, Kalous O, Reynolds CP. DIMSCAN: a microcomputer fluorescence-based cytotoxicity assay for preclinical testing of combination chemotherapy. *Methods Mol Med* 2005;110:139–53.
  44. Tognon C, Garnett M, Kenward E, Kay R, Morrison K, Sorensen PH. The chimeric protein tyrosine kinase ETV6-3 requires both Ras-Erk1/2 and PI3-kinase-Akt signaling for fibroblast transformation. *Cancer Res* 2001;61:8909–16.
  45. Stins MF, Gilles F, Kim KS. Selective expression of adhesion molecules on human brain microvascular endothelial cells. *J Neuroimmunol* 1997;76:81–90.
  46. Chao DT, Korsmeyer SJ. BCL-2 family: regulators of cell death. *Annu Rev Immunol* 1998;16:395–419.
  47. <http://www.rnidsystems.com/>.
  48. Menu E, Jernberg-Wiklund H, De Raeye H, et al. Targeting the IGF-1R using picropodophyllin in the therapeutic 5T2MM mouse model of multiple myeloma: beneficial effects on tumor growth, angiogenesis, bone disease and survival. *Int J Cancer* 2007;121:1857–61.
  49. Knezevich SR, McFadden DE, Tao W, Lim JF, Sorensen PH. A novel ETV6-3 gene fusion in congenital fibrosarcoma. *Nat Genet* 1998;18:184–7.
  50. Tognon C, Knezevich SR, Huntsman D, et al. Expression of the ETV6-3 gene fusion as a primary event in human secretory breast carcinoma. *Cancer Cell* 2002;2:367–76.
  51. Morrison KB, Tognon CE, Garnett MJ, Deal C, Sorensen PH. ETV6-3

- transformation requires insulin-like growth factor 1 receptor signaling and is associated with constitutive IRS-1 tyrosine phosphorylation. *Oncogene* 2002;21:5684–95.
52. Staerk J, Kallin A, Demoulin JB, Vainchenker W, Constantinescu SN. JAK1 and Tyk2 activation by the homologous polycythemia vera JAK2 V617F mutation: cross-talk with IGF1 receptor. *J Biol Chem* 2005;280:41893–9.
  53. Yadav A, Kalita A, Dhillon S, Banerjee K. JAK/STAT3 pathway is involved in survival of neurons in response to insulin-like growth factor and negatively regulated by suppressor of cytokine signaling-3. *J Biol Chem* 2005;280:31830–40.
  54. Staerk J, Kallin A, Royer Y, et al. JAK2, the JAK2 V617F mutant and cytokine receptors. *Pathol Biol (Paris)* 2007;55:88–91.
  55. Khan N, Mukhtar H. Multitargeted therapy of cancer by green tea polyphenols. *Cancer Lett* 2008;269:269–80.
  56. Kim J, Zhang X, Rieger-Christ KM, et al. Suppression of Wnt signaling by the green tea compound (–)-epigallocatechin 3-gallate (EGCG) in invasive breast cancer cells. Requirement of the transcriptional repressor HBP1. *J Biol Chem* 2006;281:10865–75.
  57. Imai K, Takaoka A. Comparing antibody and small-molecule therapies for cancer. *Nat Rev Cancer* 2006;6:714–27.
  58. Li M, He Z, Ermakova S, et al. Direct inhibition of insulin-like growth factor-I receptor kinase activity by (–)-epigallocatechin-3-gallate regulates cell transformation. *Cancer Epidemiol Biomarkers Prev* 2007;16:598–605.
  59. Baserga R, Peruzzi F, Reiss K. The IGF-1 receptor in cancer biology. *Int J Cancer* 2003;107:873–7.
  60. Yu H, Jove R. The STATs of cancer—new molecular targets come of age. *Nat Rev Cancer* 2004;4:97–105.
  61. Lai R, Navid F, Rodriguez-Galindo C, et al. STAT3 is activated in a subset of the Ewing sarcoma family of tumours. *J Pathol* 2006;208:624–32.